Clim Dyn (2010) 34:891–904
DOI 10.1007/s00382-009-0642-4

Tidal mixing in the Indonesian Seas and its effect on the tropical climate system

Ariane Koch-Larrouy · Matthieu Lengaigne · Pascal Terray · Gurvan Madec · Sebastien Masson

Received: 6 October 2008 / Accepted: 24 July 2009 / Published online: 9 August 2009

Abstract The sensitivity of the tropical climate to tidal mixing in the Indonesian Archipelago (IA) is investigated using a coupled general circulation model. It is shown that the introduction of tidal mixing considerably improves water masses properties in the IA, generating fresh and cold anomalies in the thermocline and salty and cold anomalies at the surface. The subsurface fresh anomalies are advected in the Indian Ocean thermocline and ultimately surface to freshen the western part of the basin whereas surface salty anomalies are advected in the Leuwin current to salt waters along the Australian coast. The $\sim$0.5°C surface cooling in the IA reduces by 20% the overlying deep convection. This improves both the amount and structure of the rainfall and weakens the wind convergence over the IA, relaxes the equatorial Pacific trade winds and strengthens the winds along Java coast. These wind changes causes the thermocline to be deeper in the eastern equatorial Pacific and shallower in the eastern Indian Ocean. The El Nino Southern Oscillation (ENSO) amplitude is therefore slightly reduced while the Indian Ocean Dipole/Zonal Mode (IODZM) variability increases. IODZM precursors, related to ENSO events the preceding winter in this model, are also shown to be more efficient in promoting an IODZM thanks to an enhanced wind/thermocline coupling. Changes in the coupled system in response tidal mixing are as large as those found when closing the Indonesian Throughflow, emphasizing the key role of IA on the Indo-Pacific climate.

A. Koch-Larrouy (✉) · M. Lengaigne · P. Terray · G. Madec · S. Masson
Laboratoire d'Océanographie et du Climat: Expérimentation et Approches Numériques (CNRS/IRD/UPMC/MNHN), case 100, Université Pierre et Marie Curie, boite 100, 4 place Jussieu, 75252 Paris Cedex 05, France
e-mail: Ariane.Koch-Larrouy@locean-ipsl.upmc.fr

G. Madec
National Oceanographic, Centre, Southampton, UK

1 Introduction

The tropical maritime continent, in the heart of the Indo-Pacific warm-pool, is a key region of the climate system. It encompasses some of the warmest surface temperatures of the world ocean that drive intense atmospheric convection (Clement et al. 2005) and is therefore able to influence climate on the global scale via atmospheric teleconnections (Neale and Slingo 2003). It also represents a passage from the tropical Pacific to the Indian Ocean, known as the Indonesian ThroughFlow (ITF), that transports $\sim$10–20 Sv of warm and fresh waters (Murray and Arief 1988; Fieux et al. 1994; Meyers et al. 1995; Gordon et al. 1999; Hautala et al. 2001; Molcard et al. 2001; Susanto and Gordon 2005; Sprintall et al. 2008). The importance of mass, heat and salt exchanges through this passage has been investigated using ocean-only (e.g., Hirst and Godfrey 1993; Murtugudde et al. 1998; Song and Gordon 2004) and coupled ocean–atmosphere models (Schneider 1998; Wajsowicz and Schneider 2001; Song et al. 2007) by contrasting ITF-on and off experiments. These studies have demonstrated the importance of the ITF in modulating the Indo-Pacific oceanic mean state. By carrying waters from the western Pacific to the Indian Ocean, the ITF is shown to warm and fresh the upper Indian Ocean while cooling and salting the upper Pacific Ocean. In addition to these direct oceanic effects, CGCMs results have also highlighted the role of the ITF in regulating the position of the atmospheric deep convection and thereby the surface wind and pressure patterns (Song et al. 2007).

Besides its critical role in transferring mass, heat and salt between the Pacific and Indian warm pools, the Indonesian Archipelago (IA) is also a region of strong water mass transformation. It is indeed the only region of the world where strong internal tides remains trapped in the semi enclosed seas, so that a large amount of tidal energy remains available for vertical mixing (Koch-Larrouy et al. 2007, 2008a, hereafter KL07 and KL08a). Estimates of the vertical diffusivity are ten times larger than in the open ocean (Ffield and Gordon 1992; Hautala et al. 1996; Ffield and Gordon 1996). In most models, this mixing is not taking into account, and the ITF water masses remain as stratified as the Pacific ones (e.g. Kamenkovich et al. 2003; Gordon and McClean 1999). In particular, recent studies pointed out the importance of this additional vertical diffusivity on Indonesian water masses and for remote TS properties (Potemra et al. 1997; Schiller et al. 1998; Schiller 2004, KL07, KL08a, KL08b). In an ocean-only model, KL07 developed a specific parameterization to represent the effect of tidal mixing in the IA, providing a 4D (space and time) vertical tidal diffusivity. This study demonstrates that taking into account tidal mixing allows a good representation of the mean vertical diffusivity and of the water masses in all the different seas of the archipelago. This additional mixing is responsible for the Pacific water transformation into the Indonesian Throughflow Water, which is characterized by a fresher and colder thermocline and an isohaline layer. This layer formation results from the mixing of surface and intermediate fresh waters with saltier pacific subtropical waters (Koch-Larrouy et al. 2008b, hereafter KL08b). It is the only region of the tropical band to allow such a surface buoyancy penetration, owing to this near-surface tidal mixing (KL08a). This Indonesian tidal mixing cools the sea surface temperature (SST) by $\sim$0.5°C and allows the ocean to absorb an additional heat flux of $\sim$20 W/m^2. Such an SST change in a region of deep atmospheric convection is likely to affect the climate system. A recent study (Jochum and Potemra 2008, hereafter JP08) using a Coupled General Circulation Model (CGCM) demonstrate the significant influence of a constant enhanced vertical diffusivity (1 cm^2/s) in the Java-Flores and Banda Seas on the tropical precipitation. However, they did not study the influence of this additional mixing on the tropical Indo-Pacific variability. Moreover, our experimental design allows to account for the spatial heterogeneity of vertical diffusivity in the Indonesian region consistently with observations (e.g. Ffield and Gordon 1996; Robertson and Ffield 2005, KL07; Schiller and Fiedler 2007).

The goal of this study is therefore to further document the impact of an heterogeneous tidal mixing within the IA on the tropical climate both in term of mean state and variability using a CGCM. The model and the tidal parameterization used are described in Sect. 2. The results on the ocean and atmosphere mean states are investigated in Sect. 3, whereas changes in variability are discussed in Sect. 4. Finally Sect. 5 gives the main conclusions, discusses the robustness of the results and proposes some perspectives to this work.

2 Experimental setup

The model used in this study is the HadOPA global coupled ocean–atmosphere model. Details of model formulation are documented in Lengaigne et al. (2004). Only a brief description of the coupled model configuration is provided here. A description the tropical climate simulated by this model can be found in Lengaigne et al. (2004, 2006).

The ocean component of HadOPA coupled model is OPA8.2 model in its global configuration, known as ORCA2. The horizontal mesh is based on a 2° × 2° Mercator grid, with a refinement of the meridional resolution in the tropics, allowing a 0.5° resolution at the equator. The grid features two points of convergence in the Northern Hemisphere, both situated on the continent. The model has 31 levels with 14 lying in the top 150 m. Vertical eddy viscosity and diffusivity coefficients are computed from a 1.5 turbulent kinetic energy closure scheme (Blanke and Delecluse 1993). This OGCM has been extensively validated in uncoupled mode in the tropics where it closely matches the observations (e.g. Vialard et al. 2001; Lengaigne et al. 2003; Cravatte et al. 2007). There is no interactive sea–ice model in this configuration: sea–ice cover is specified from an observed monthly climatology.

The atmospheric component is the HadAM3 atmospheric model (Pope et al. 2000). The model has a horizontal resolution of 3.75° longitude × 2.5° latitude, with 19 levels in the vertical. Convection is parameterized using the mass-flux scheme of Gregory and Rowntree (1990), with the addition of convective momentum transport (Gregory et al. 1997). The quality of the AGCM simulation of ENSO has been studied extensively by Spencer and Slingo (2003) who showed that in the tropics, the UM reasonably captures the associated precipitation and large-scale circulation anomalies.

These oceanic and atmospheric components are coupled through OASIS 2 coupler (Valcke et al. 2000). Fluxes between these components are exchanged every day, without flux correction.

The role of the Indonesian tidal mixing on the tropical climate is investigated in this coupled model by adding a tidal mixing parameterization to the vertical mixing over the semi enclosed seas of the IA. This parameterization is

identical to the one described in KL07 and provides a 4D (space and time) vertical tidal diffusivity. The function of energy transfer between baroclinic and barotropic tides is inferred from a tidal model (Lyard et al. 2002), ensuring the right amount of energy input and its correct horizontal structure whereas the energy vertical profile is inferred from an internal tide generation model (Gerkema et al. 2004), allowing a maximum energy dissipation in the thermocline. The very good agreement with TS structure within all subseas of the archipelago (KL07) therefore allows us to confidently use the horizontal and vertical diffusivity prescribed.

The sensitivity of the tropical climate to this tidal mixing is assessed by comparing three experiments using different tidal energy forcing in the Indonesian archipelago. The reference experiment (HnoT) has a zero tidal energy input (no tidal mixing) and is thus identical to Lengaigne et al. (2004) experiment. The two other experiments use the same tidal energy forcing as in KL07 (HT) and twice the energy forcing (H2T). The latter experiment allows documenting the climate sensitivity to the magnitude of the tidal mixing. The doubled tidal energy still remains within the range of the uncertainties of tidal energy estimates in the region (Lyard and Robertson, personal communication). All these experiments have been run for 200 years starting from the same initial state (the last time step of another 100-year run) and results are displayed for the last 100 years.

In Sect. 3, the statistical significance of the correlation/regression coefficients have been assessed with a phase-scrambling bootstrap test (Davison and Hinkley 1997). No filtering is applied to the various simulated fields prior to statistical analysis.

3 Tidal mixing effect on the mean state

The 15 Sv ITF transport calculated for HnoT experiment agrees well with other ocean-only and coupled models (e.g. Potemra and Schneider 2005; Meng et al. 2004; Koch-Larrouy et al. 2007; Song et al. 2007), the SODA product and with the most recent estimates inferred from observations, even if slightly underestimated. Indeed, the latest long-term simultaneous measurements within both inflow and outflow passages (INSTANT 2004–2006) estimated a total transport of 14 $\pm$ 3 Sv (Sprintall et al. 2008), larger than previous estimates (10 Sv, Gordon and Susanto 2001). The simulated flow is composed by 11.8 Sv coming from the western route and 3.2 Sv from the eastern route, in good agreement with recent observations (respectively, 11.5 $\pm$ 2 and 2.5 $\pm$ 1 Sv, Sprintall et al. 2008). The introduction of tidal mixing reduces by $\sim$1 Sv the total transport, mainly along the eastern route. A similar effect was found in KL08a forced experiments. It constrasts with JP08 results who did not find any change in the transport. This might be due to the difference in the localisation of the mixing and/or the difference model used.

Taking into account tidal mixing considerably improves the water mass properties at the exit of the IA (Fig. 1). In the two entrance seas (North and South Pacific, blue and red points), the simulated characteristics of the water masses are very similar between the different experiments. The simulated thermocline structure displays a salinity maximum associated to Pacific subtropical waters and a salinity minimum associated to the North Pacific intermediate water masses (NPIW), as in the observations. Nevertheless, the simulated salinity maximum of the North Pacific Subtropical Water (NPSW) is overestimated by $\sim$0.5 psu due to an excess of evaporation in the subtropical gyre where the water mass is formed. In HnoT simulation, as in most models without tidal mixing (Gordon and McClean 1999; Schiller et al. 1998; Sasaki et al. 2008; Schiller 2004), the water masses remain almost unchanged during their journey through the Archipelago. The IA mainly acts as a transfer pipe of waters from the Pacific into the Indian Ocean without any transformation. This feature does not match the observations and simulations including tidal mixing (Schiller et al. 1998; Schiller 2004, KL07, KL08a, KL08b, JP08), where the salinity maxima are eroded within the Indonesian archipelago, resulting in a halinstad thermocline layer in the Indonesian ThroughFlow Water (ITW). The tidal mixing prescribed in HT

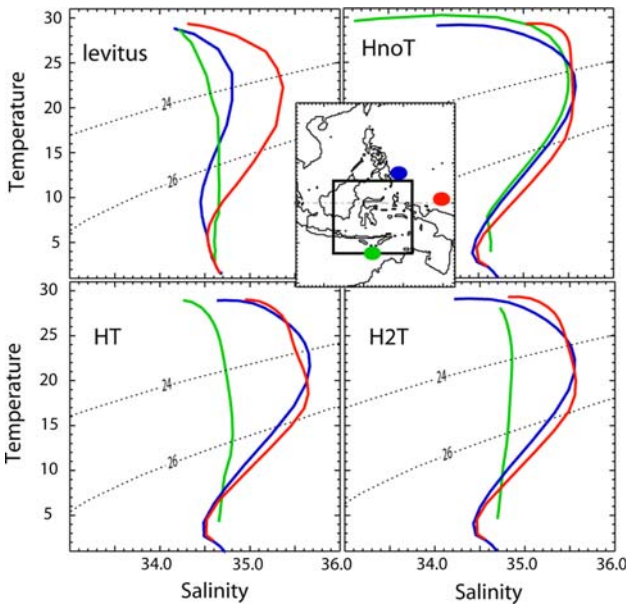

Fig. 1 TS diagrams for the HnoT, HT and H2T experiments (see Table 1) and LEVITUS data set, in the entrance (*blue* North Pacific and *red* South Pacific) and at the exit (*green* Australian basin). Neutral density 24 and 26 are overplotted in *dashed line*

Table 1 Set of experiments

	S-noTi	S-Ti	H-noTi	H-Ti	H-2Ti
Atmosphere model	ECHAM T106	ECHAM T106	HADAM T42	HADAM T42	HADAM T42
Ocean model	OPA 0.5°	OPA 0.5°	OPA 2°	OPA 2°	OPA 2°
Tidal mixing param	No	Yes	No	Yes	Yes
Tidal mixing energy	–	1	–	1	2

experiment allows a realistic erosion of the Pacific subtropical waters, therefore considerably improving the ITW properties compared to HnoT. However, the halinstad layer simulated in HT is slightly too salty, due to the aforementioned excess of salt content in the NPSW. Vertical eddy diffusivity coefficient averaged over the Indonesian archipelago in HT experiment (1.5 cm^2/s; Table 2) also agrees with estimates inferred from observations using simple advection/diffusion models (1–3 cm^2/s, Ffield and Gordon 1992) and with the one obtained in the ocean only experiments (1.5 cm^2/s; Table 2). The improved water mass properties and the realistic vertical diffusivity coefficients when parameterizing tidal mixing give us confidence in results discussed in the following.

Tidal mixing strongly modifies the temperature and salinity profiles in the Indonesian Archipelago (Fig. 1). Thermocline water masses (i.e. waters between the neutral density 24 and 26, that is between ~100 and 200 m), are freshened by ~0.3 psu and cooled by ~1°C (Fig. 2). Vertical mixing erodes the salinity maximum and acts to transfer cold water from below into the thermocline and the surface. These fresh and cold thermocline anomalies are advected by the ITF and by the Indian South Equatorial Current, resulting in a strong salinity and temperature signature in the North and Western Indian Ocean thermocline (Fig. 2).

In addition to the subsurface properties, tidal mixing also strongly influences the surface properties of the Indonesian region. Surface temperatures in the reference experiment display a significant (larger than the warm pool uncertainties, see Hurrel and Trenberth 1999) warm bias (Fig. 3, 28.5°C isotherm position and Table 2 for three observational data sets), as other coupled models. This bias results in an overestimation of deep convection over the IA as in many other coupled models (Lin 2007) and therefore an excess of precipitation over the IA and over the northwestern tropical Pacific and the South China Sea when compared to observations (Fig. 3; Table 2 for two observational precipitation data sets). The inclusion of tidal mixing acts to strongly reduce these biases by mixing surface warm waters with colder waters from below (Fig. 3; Table 2), producing a mean cooling over the maritime continent by ~0.5°C. The associated SST bias found in HnoT experiment is significantly reduced (Table 2). Furthermore, it considerably improves both the structure and the amplitude of the precipitation over the IA, with a 20% reduction of the precipitation amount over the archipelago (−1.5 out of 7.5 mm/day annual mean, see Table 2). The amplitude are reduced around 120°E (Fig. 3; Table 2) and over the Java Sea, in better agreement with observations. The structure patterns are quite similar for

Table 2 Average quantities anomalies over the Indonesian archipelago (box shown in Fig. 4) between F-Ti and F-noTi for the forced KL07's model, between S-Ti and S-noTi for the SINTEX model and between H-Ti and H-noTi and also between H-2Ti and H-noTi for the HadOPA model

	F-Ti-F-noTi	S-Ti-S-noTi	H-Ti-H-noTi	H-2Ti-HnoTi
Kz tides (cm^2/s)	+1.5	+1.7	+1.5	+3
SST (°C)	−0.5	−0.45	−0.5	−0.85
SSS (psu)	−0.02	+0.2	+0.7	+1.4
Heat uptake (W/m2)	+19	+21.7	+18	+34
Rain (mm/day)	–	−1.5	−1.5	−2.4

Table 3 Average quantities over the Indonesian archipelago in the box shown Fig. 4 for the S-noTi, S-Ti, H-noTi, H-Ti and H-2Ti experiments and the Observations : Kz (Ffield and Gordon 1992), SST (Levitus, Reynolds and HadISST) and SSS (Levitus) and CMAP, GPCP and TRMM for the precipitations

	S-noTi	S-Ti	H-noTi	H-Ti	H-2Ti	OBS		
Kz tides (cm^2/s)	0	1.7	0	1.5	3	1-2		
SST (°C)	30	29.55	29.45	28.95	28.6	Lev 28.5	Rey 28.8	Had 28.5
SSS (psu)	33.0	33.2	33.15	33.85	34.55	33.9		
Rain (mm/day)	6.9	5.4	7.4	6	5	CMAP 5.4	GPCP 4.1	TRMM 5.3

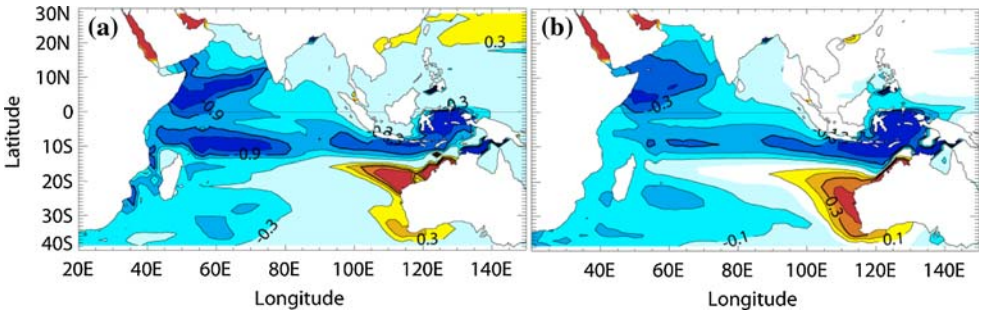

Fig. 2 Differences between HT and HnoT experiments average between the neutral density 24 and 26 (thermocline layer, about 100–200 m) for **a** temperature and **b** salinity. Differences that are below the 99% confidence level estimated with a Student's *t* test are masked

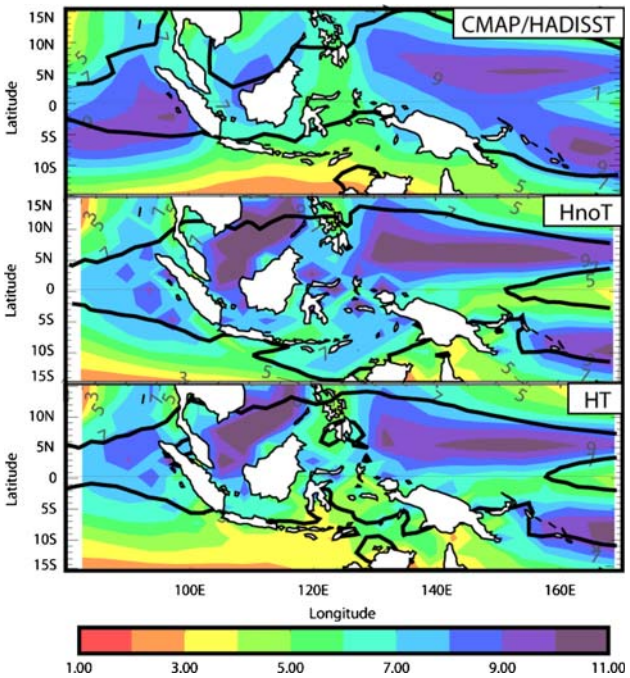

Fig. 3 Annual average of precipitation with overlayed in *black* the 28.5 isotherm for the observations (CMAP, 1979–2004, and HADISST, 1950–2006) and H-noTi, H-Ti experiments (from top to bottom)

both the winter and the summer season (not shown), in contrast to what have been found in JP08.

The weakening of the convective activity over the IA results in an ocean heat uptake of 18 W/m^2 (Table 2). This net heat flux anomaly is driven by both an increase of solar radiation (6 W/m^2) thanks to a reduced cloud cover and a positive latent heat flux anomaly (12 W/m^2) due to decreased evaporation. Whereas the net heat flux entering the ocean is weak in the HnoT experiment ($\sim$10 W/m^2), it becomes comparable to the heat gain in the Western central Pacific when including tidal mixing (30 W m^{-2}). The net heat flux and the SST anomalies generated by tidal mixing in this coupled framework are very similar to the one found in the ocean-only experiments (KL07 and Table 2). In contrast, the SSS anomaly generated in the coupled experiments largely exceeds the one simulated in the ocean-only simulations (0.7 vs. 0.04 psu, Table 2). The weak ocean-only response is related to the absence of atmospheric feedback (no reduction of precipitation) and to the restoring to the observed surface salinity applied in the forced experiments. In the coupled simulation, both vertical mixing of salty subtropical waters and the weaker local precipitation act to increase the SSS. However, the effect of tidal mixing on SSS is presumably overestimated in this coupled model due to the overestimation of the salinity maximum in the NPSW. These saltier surface waters are then advected into the Leuwin current, subduct between 15°S and 20°S and thus salt the thermocline along the Australian coast (Fig. 2).

Tidal mixing in the IA impacts the coupled system not only locally but also in the entire tropical Indo-Pacific region (Fig. 4). The SST cooling in the IA redistributes the global tropical precipitation. The tropical deep convection shifts away from the maritime continent. The precipitation loss over the IA is compensated by increased rainfall over the western equatorial Indian and Pacific Oceans and in the northern part of the Philippine Sea. Furthermore, the annual mean InterTropical Convergence Zone is slightly shifted southward. The increased rainfall over the western Pacific freshens the western Pacific warm-pool (−0.2 psu). The increased precipitation over the western Indian Ocean is responsible of 1/3 of the surface freshening in that region. The remaining 2/3 is attributed to the subsurface fresh anomalies generated in the IA, advected toward the western Indian ocean (Fig. 2b) and then upwelled in the elongated 10°S thermocline dome and the Somali current (Fig. 4 bottom).

The decreased convective activity over the Indonesian region also leads to a reduction of low-level convergence wind in HT experiment. The trade winds relax in the central Pacific ($\sim$+10%) whereas winds along the Java Coast strengthen ($\sim$+30%) (Fig. 5). The Pacific trade winds relaxation reduces the equatorial upwelling, flattens the equatorial Pacific thermocline (Fig. 5) and warms the central Pacific by $\sim$0.5°C (Fig. 4). In contrast, the stronger along Java coast winds re-enforced the Java upwelling, shoals the thermocline (Fig. 5) and cools the SST in this region (Fig. 4).

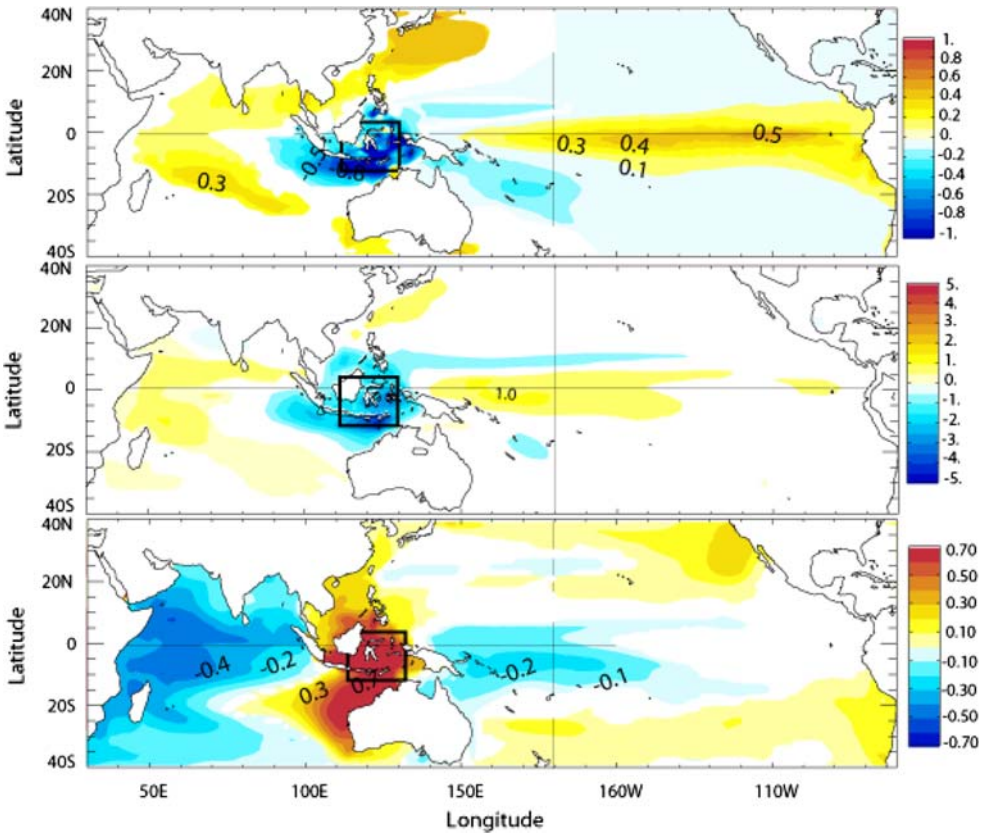

Fig. 4 Differences between HT and HnoT experiment for *top* SST (°C), *middle* rain (mm/day) and *bottom* SSS (psu). Differences that are below the 99% confidence level estimated with a Student's *t* test are masked

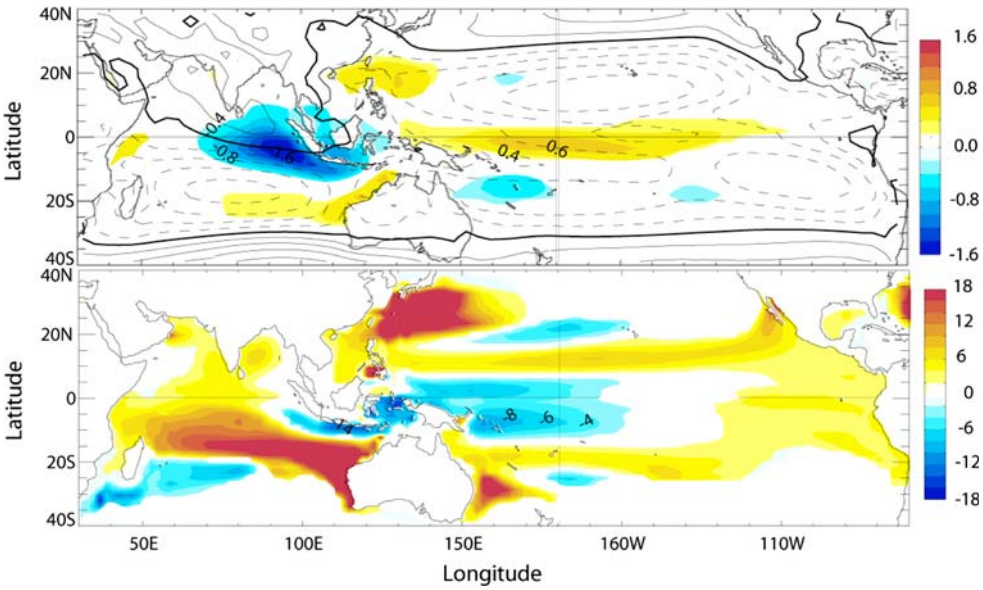

Fig. 5 Zonal wind (m/s, *top panel*) and thermocline depth (m, *bottom panel*) anomalies between the HT and HnoT experiments. Differences that are below the 99% confidence level estimated with a Student's *t* test are masked. *Contour lines* on top panel shows the annual mean zonal wind. *Solid* (resp. *dashed*) *thin lines* represent mean zonal wind toward the east (resp. west). *Thick line* is the zero line. Contour intervals are every 2 m/s

The relationship between the intensity of the internal tidal energy in the IA and its local effect is mainly linear. Doubling the internal tidal energy (H2T experiment) doubles the mean vertical diffusivity (Table 2). Salinity anomalies are also doubled whereas local precipitation and SSTs anomalies increase only by a factor 1.7 (Table 2), suggesting a weak non-linearity between Kz and SST, presumably due to atmospheric coupled feedback. The Kz, SST and heat fluxes anomalies found in JP08 (mean vertical diffusivity of 1 cm^2/s) are 2/3 smaller than the one found in this study in good agreement with a quasi linear response between them. Both the precipitation and SST mean values over the IA in H2T remain in good agreement with observations (Table 2). The remote precipitations and

SST anomalies increased between HT and H2T and their structure are relatively similar (not shown).

4 Tidal mixing effect on the variability

Tidal mixing not only affects the mean state of the tropical Indo-Pacific system but also its interannual variability. Figure 6 shows the standard deviation of SST anomalies for the HnoT experiment and the differences with the HT and H2T experiments. The SST variability is globally enhanced (decreased) in regions where thermocline shoals (deepens) in HT experiment (compare Figs. 5, 6). The central and eastern Pacific interannual signal is hence weakened. Table 4 confirms that El Nino Southern Oscillation (ENSO) amplitude is reduced by $\sim$10% in the HT and H2T experiments slightly reducing a long standing bias in this coupled model (Lengaigne et al. 2006). The H2T and HT ENSO amplitudes are similar suggesting that the relationship between the ENSO amplitude and the kz/SST/rain over the maritime continent is not linear, mainly due to different wind/thermocline anomaly structure in the Pacific Ocean (not shown). Both these reductions are of the same order of magnitude as the one found when contrasting the ITF on and off (Song et al. 2007). The interannual SST variability over the Indian Ocean is also affected by tidal mixing with a large increase (15% see Table 4) in the South Eastern Tropical Indian Ocean (SETIO, 90–110°E, 10–0°S), recognized as one of the action centers of the Indian Ocean Dipole/Zonal Mode (IODZM, e.g., Saji et al. 1999; Webster et al. 1999; see Chang et al. 2006 for a review).

The other characteristics of ENSO (spectral characteristics, asymmetry, seasonal phase locking, SST precursors) remain unchanged (see Table 4), in contrast to what has been found in ITF-off experiments (Song et al. 2007). On the other hand, the IODZM shows significant changes in addition to the increased interannual SST variability when including tidal mixing. There are two positive feedbacks involved in the IODZM, one being the Bjerknes-type wind-thermocline-SST feedback, the other being a positive feedback between the wind, evaporation, and SST (Li et al. 2003). Both of these positive feedbacks take place over the SETIO from boreal spring to fall. We argue that the

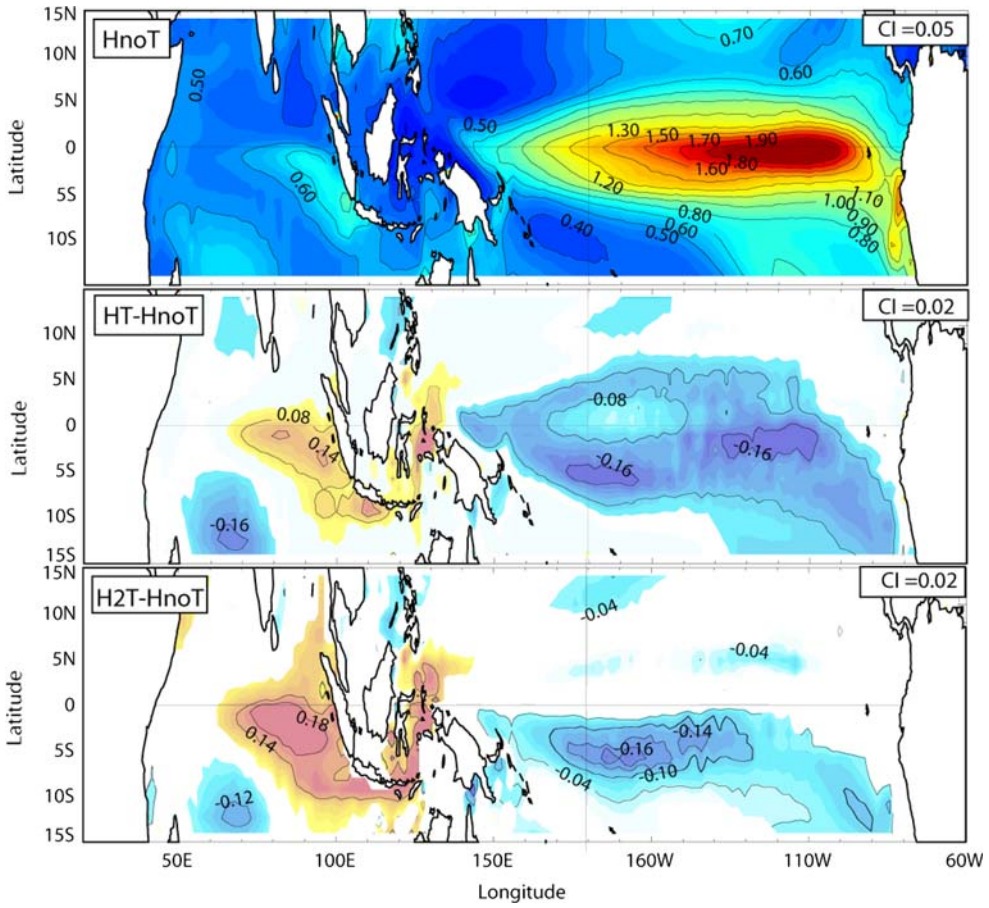

Fig. 6 Standard deviation of SST for *top* the HnoT experiment and *middle* the difference between HT and HnoT and *bottom* the difference between H2T and HnoT for the last 100 year. Differences that are below the 99% confidence level estimated with a Student's *t* test are masked

Table 4 RMS and skewness of the Niño-34 SSTs index, RMS of SETIO SSTs index, correlation between the SETIO SSTs and the SETIO thermocline anomalies, correlation between the SETIO SSTs and the SETIO zonal wind anomalies, correlation between the Niño-34 SSTs and the Oct–Nov SETIO SSTs at the peak period and at the previous winter period

	H-noTi	H-Ti	H-2Ti	Obs
RMS Niño-34 SST (°C)	1.29	1.14	1.13	0.8
Niño-34 Skewness	0.45	0.44	0.32	0.6
RMS SETIO SST (°C)	0.7	0.82	0.94	0.45
Corr. between Niño-34 and Oct–Nov SETIO SSTs	0.7	0.6	0.6	0.6
Corr. between the previous winter Niño-34 and Oct–Nov SETIO SSTs	0.	−0.3	−0.5	−0.3

We use the Niño-34 index (SST averaged over the area 5°S–5°N, 170–120°W) as a proxy for ENSO variability. Using the Niño-3 index does not change the results. The SETIO domain is 90–110°E, 10–0°S and is used as a (negative) indice of a positive phase of IODZM. The observed values are deduced from the HADISST data set

shallower SETIO thermocline in HT experiment favors the wind-thermocline-SST feedback during boreal fall and increase the sensitivity of the coupled IODZM system. In order to support this hypothesis, we have diagnosed the strength of the wind-thermocline-SST feedback in the experiments by correlating key-variables involved in this coupling (see Table 5). The correlation between the SST and thermocline depth anomalies in the SETIO region, as well as the correlation between equatorial zonal wind and SETIO thermocline depth anomalies increase with tidal mixing in October–November. Similarly, the correlation between equatorial zonal wind and SETIO SSTs increase one month lagged (see Table 5). Also consistent with a stronger wind-thermocline-SST feedback, there is a region of stronger rainfall standard deviation during boreal fall (not shown), collocated with the region of higher SST variability (e.g. the SETIO, Table 4). The enhanced coupled variability in the SETIO region may then be attributed to an enhanced atmospheric/thermocline coupling due to a shallower thermocline. Similar findings have been discussed in Song et al. (2007) when closing the ITF.

In the literature, the IODZM has been seen to be significantly correlated to the Pacific ENSO during boreal fall (Fischer et al. 2005; Chang et al. 2006). Tidal mixing does not modify this seasonally phase-locked relationship between the two phenomena since the correlations between Indo-Pacific SST anomalies and the SETIO time series during boreal fall do not change significantly with tidal mixing (Fig. 7 right panels). The correlation coefficient between Nino34 and SETIO indices confirms 30% of co-occurrences between these two phenomena with or without tidal mixing (Table 4).

Table 5 Correlation between the SETIO SSTs and the SETIO thermocline anomalies, between the equatorial (2°S–2°N, 70°E 90°E as in Fischer et al. 2005) zonal wind and the SETIO thermocline anomalies and between equatorial zonal wind and the SETIO SSTs at the peak period (ON) of IODZM and for the entire time series

	H-noTi		H-Ti		H-2Ti	
	Annual	ON	Annual	ON	Annual	ON
SETIO SST and SETIO D20	0.59	0.82	0.67	0.89	0.68	0.96
EQ wind and SETIO D20	0.79	0.86	0.81	0.91	0.82	0.92
EQ zonal wind and SETIO SST	0.62	0.94	0.73	0.94	0.74	0.94

Correlations are all above the 99% confidence level estimated with a phase-scrambling bootstrap test with 999 samples

Despite of considerable efforts, it is yet unclear what triggers the initial wind and SST anomalies of IODZM and how much of those are intrinsic to the Indian Ocean (Chang et al. 2006). Figure 7 (left panels) shows the lag-correlations between the SETIO time series during boreal fall and the Indo-Pacific SSTs one year before for the HnoT, HT, H2T experiments and observations. Including tidal parameterization changes the ENSO influence on the IODZM and its predictability: the SST precursors of IODZM events, one year before the peak phase of the events are considerably modified with the inclusion of tidal parameterization in the IA. For the reference simulation (HnoT), the SST precursors of a SETIO cooling event (positive phase of the IODZM) are hardly significant and concern only positive anomalies in the central extra-equatorial Pacific and negative SSTs in the Indian Ocean (Somalia coast, Bay of Bengual, Leuwin current, China Sea and ITF). When including tidal mixing (HT), these precursors show a significant La Niña-like pattern with negative eastern equatorial Pacific SSTs and South Eastern Indian Ocean (SEIO: black box Fig. 8) SSTs in better agreement with observations. More precisely, including tidal mixing improves the correlation between the previous ENSO and the SETIO events (see Table 4). When doubling tidal mixing (H2T), these precursors are reinforced, demonstrating the robustness of the effect of tidal mixing on the relationship between IODZM and ENSO in this model (Fig. 7; Table 4).

We can wonder why the SEIO and eastern equatorial Pacific negative SST anomalies are significant statistical

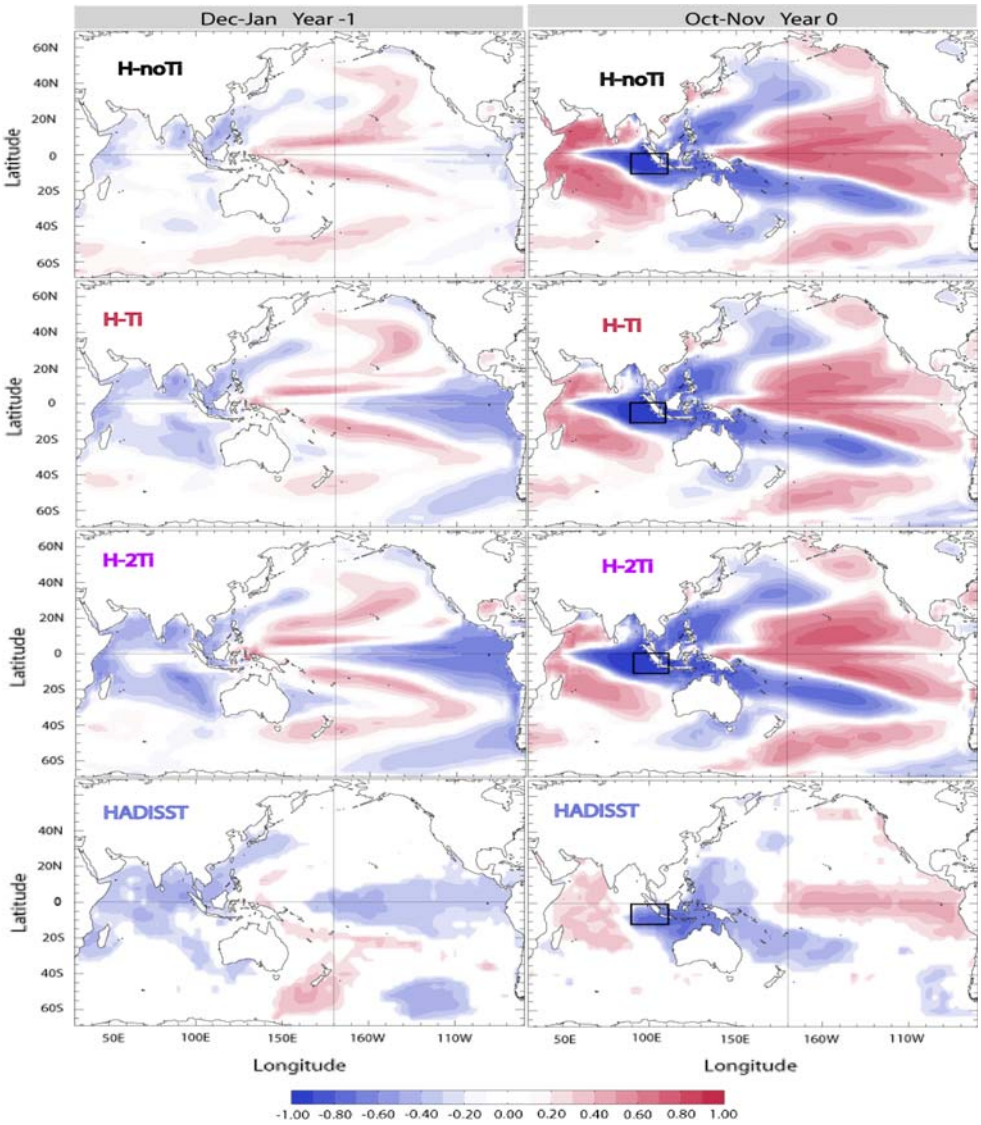

Fig. 7 Time sequence of correlations with October–November negative SETIO (90–110°E, 10–0°S) SST time series of Indo-Pacific SSTs, as an index for the IODZM computed from the HnoT (*top*), HT (*second line panels*), H2T (*third line panels*) and the HADISST (1950–2004, bottom). The correlations are computed with the negative SETIO time series so that the polarity is consistent with the occurrence of a positive IODZM event. *Left panels* December–January before October–November SETIO cooling SST (i.e. 5 bimonthly seasons before), and *right panels* at the same period than October–November SETIO SST (i.e. during the peak of the positive IODZM event). Correlations that are above the 90% confidence level estimated with a phase-scrambling bootstrap test with 999 samples are *shaded*; otherwise the plot is *left blank*. The *black box* on the left panels shows the SETIO domain

precursors of an IODZM event and re-enforced by Indonesian tidal mixing. Figure 8 shows that these SST precursors are generated in the maturing phase of La Niña during boreal winter (December–January). Consistent with the co-occurence of IODZM and El Niño several months later (Fig. 7, left panels), one can also observe on Fig. 8 a large anomalous cyclonic circulation over the northwestern Pacific which bears a strong resemblance with the Philippine Sea (El Niño) onset cyclone described in Wang (1995) as a key precursor to ENSO events during recent dedades. Turning now to the Indian Ocean variability, the excess of precipitation over the maritime continent and western Pacific are associated with the rapid growth of low-level cyclonic anomalies on both sides of the equator over the eastern Indian Ocean. This suggests that the cyclonic circulation over the eastern Indian Ocean developed as a Matsuno-Gill type response to enhanced convective heating over the Maritime continent during La Niña years. Consistent with the existence of a positive wind-evaporation-SST feedback, the southeasterly wind anomalies between 25 and 10°S associated with this cyclonic circulation are collocated with increased evaporation over the SEIO, since the climatological winds are also southeasterly over this area during February–March (not shown). This leads to surface cooling through enhanced latent heat fluxes associated with the increase of the total wind speed. Once generated, the SEIO negative SSTs are responsible for the generation of the IODZM event by coupled wind and SST anomalies propagating northward (Murtugudde et al. 2000; Gualdi et al. 2003; Terray et al. 2007). The reason for the northward propagation of these coupled anomalies has been discussed in details by Terray et al. (2007). All the anomalies are clearly enhanced with (doubling) tidal mixing. Including tidal mixing, by upwelling and

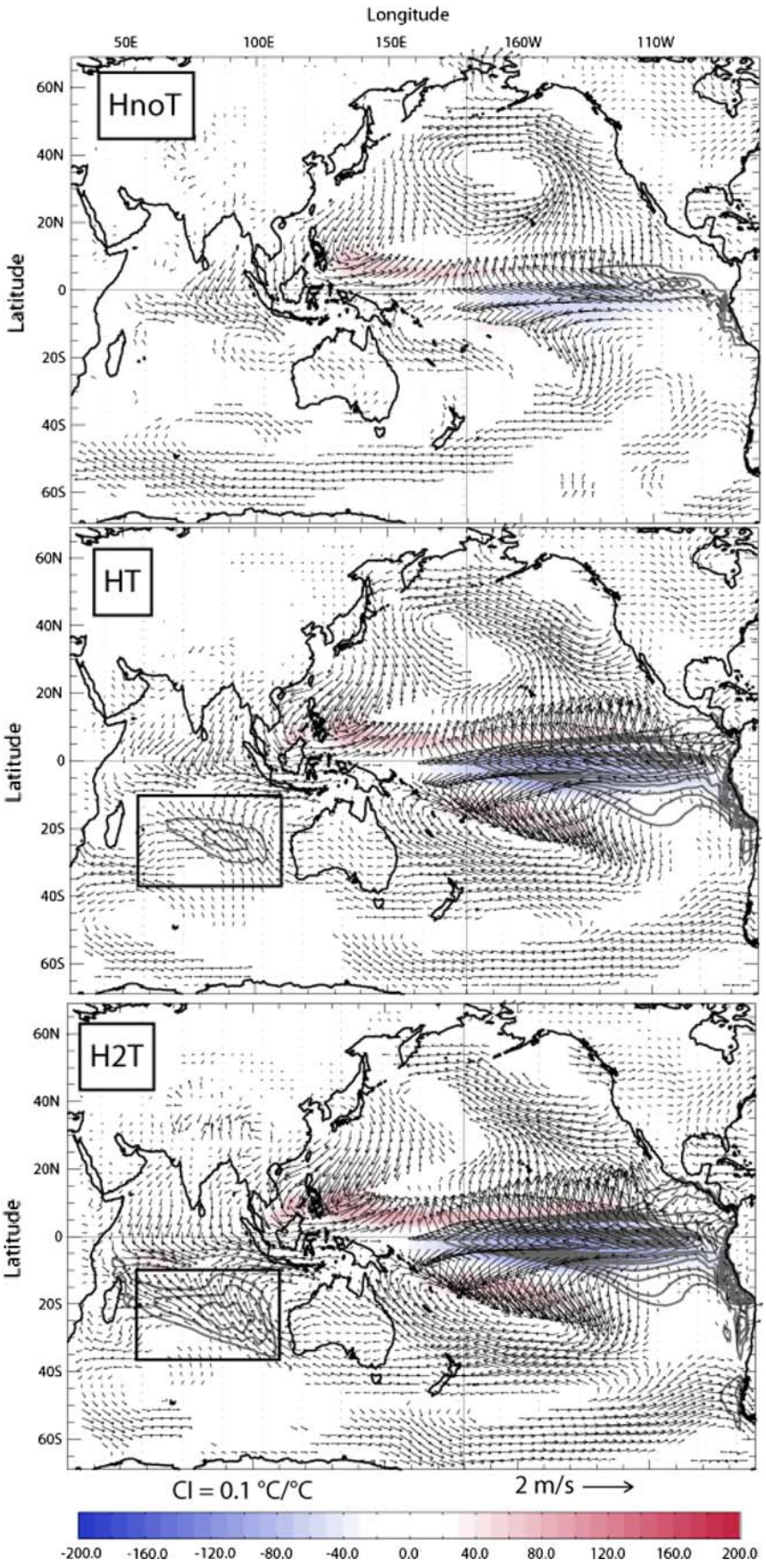

Fig. 8 December–January regression coefficients of Indo-Pacific 850 hPa wind (*arrows* see scale below the panels, m/s by STD), SST (*grey contours*, CI = 0.2°C by STD) and precipitations (*colours shading*, CI = 10 mm/month by STD) versus the October–November negative SETIO (90–110°E, 10–0°S) SST time series computed from the HnoT (*top*), the HT (*middle*) and the H2T (*bottom*) experiments. Note that the regression coefficients have been computed with the negative SETIO time series to be consistent with Fig. 7. The units labelled in all the regression patterns are actually the units per standard deviation of the index being regressed (e.g. SETIO time series).The *black box* shows the SEIO domain (55°–110°E and 10°–37°S)

shallowing the thermocline in the SETIO region, allows these anomalies to be more efficient in promoting an IOD-ZM event several months later.

5 Conclusion/discussion

In the Indonesian archipelago, strong internal tides are trapped in the semi-enclosed seas, resulting in a considerable thermocline mixing that modifies the Pacific stratification and surface properties before entering the Indian Ocean. The effect of this tidal mixing on the tropical climate system has been investigated using a climate model including a non-uniform and energy constrained parameterization with two different tidal energy forcings within the range of uncertainties.

Taking into account tidal mixing considerably improves water masses properties and vertical diffusivity in the Indonesian archipelago. It mixes thermocline waters with below and upper water masses in this region, generating fresh and cold anomalies in the thermocline ($\sim$0.3 psu and $\sim$1°C) and salty and cold anomalies at the surface ($\sim$0.7 psu and $\sim$0.5°C). The resulting changes in the haline structure within the archipelago affect the whole Indian Ocean: subsurface fresh anomalies are advected in the western part of the basin, surface via coastal upwelling and induces a surface freshening of the western Indian Ocean while surface salty anomalies are advected by the Leuwin current salt the thermocline along the western Australian coast.

The surface cooling over the Archipelago reduces by 20% the overlying deep atmospheric convection. It improves both the amount and the structure of the rainfall over this region and increases by 20 W/m^2 the ocean heat uptake. The associated wind convergence over the maritime continent is then reduced and the pacific trade winds relax while summer winds along Java coast strengthen. These wind changes deepen the eastern Pacific thermocline, warming the associated equatorial upwelling region, and shoal the western Pacific and eastern Indian Ocean thermocline.

These mean state changes are in good agreement with JP08 study, using a different model and a constant vertical diffusivity only in the Banda-Flores and Java Sea. Moreover, they shown to be mainly linear when doubling the magnitude of tidal mixing, as well as comparing them to the smaller mixing introduced in JP08. Moreover, similar experiments with and without tidal mixing performed with another coupled model using a different atmospheric component and higher atmospheric and oceanic resolution also confirm the robustness of the tidal mixing effect on the tropical mean climate (see Appendix). They seems very robust from one model to another. However, the JJA and DJF are only slightly different in our study in contrast to JP09's results. This suggests that either the model or the vertical diffusivity prescription (larger and heterogeneous in our model) may modify the seasonal response, for which others experiments would be required in order to conclude on that matter.

Tidal mixing in the IA also affects the tropical Indo-Pacific variability. The SST variability is shown to respond to the changes in thermocline depth. In the Pacific, the deepening of the thermocline acts to slightly damp ENSO variability (10%) while the shallower thermocline in the eastern Indian Ocean leads to a 15% increase of IODZM variability. Furthermore, the relationship between the IOD-ZM and ENSO are significantly changed. IODZM are more strongly influenced by ENSO variability in the preceding winter. In the coupled model, the SEIO precursors are actually related to ENSO events one year before the IOZM peak. Thanks to an enhancement of the wind/thermocline coupling in the SETIO region, SETIO precursors becomes more efficient in promoting an IODZM. In other coupled models (Fischer et al. 2005; Lau and Nath 2004), SETIO precursors are multiple and not only related to ENSO phenomena (e.g. connected to extratropical variability in the Southern Ocean). The enhanced wind/thermocline coupling when including Indonesian tidal mixing in these models, is also likely to any precursors of the IODZM. The diversity of SETIO precursors and the sensitivity of these precursors to tidal mixing suggest that the predictability of the IODZM discussed in Song et al. (2007) could strongly depend on the model and the physical parameterization used.

This study therefore suggests that tidal mixing in the ITF is an important component for both the mean state and the variability of the Indo-Pacific region. The amplitude of the changes related to the inclusion of tidal mixing are of the same order as those generated when closing the ITF (Song et al. 2007). Mixing in this region seems to be as important as the fresh and warm transfer via the Indonesian region on the climate system. Coupled climate models should hence include the effect of this tidal mixing in order to refine their simulation.

Appendix

SINTEX F1 coupled model

The other model used in this paper is an upgraded version of SINTEX-F1 ocean atmosphere coupled model (Luo et al. 2003, 2007). This new version has been developed in a frame of EU-Japan collaborations between LOCEAN, MPImet and FRCGC. Its oceanic component is NEMO (http://www.locean-ipsl.upmc.fr/NEMO) with OPA9.2

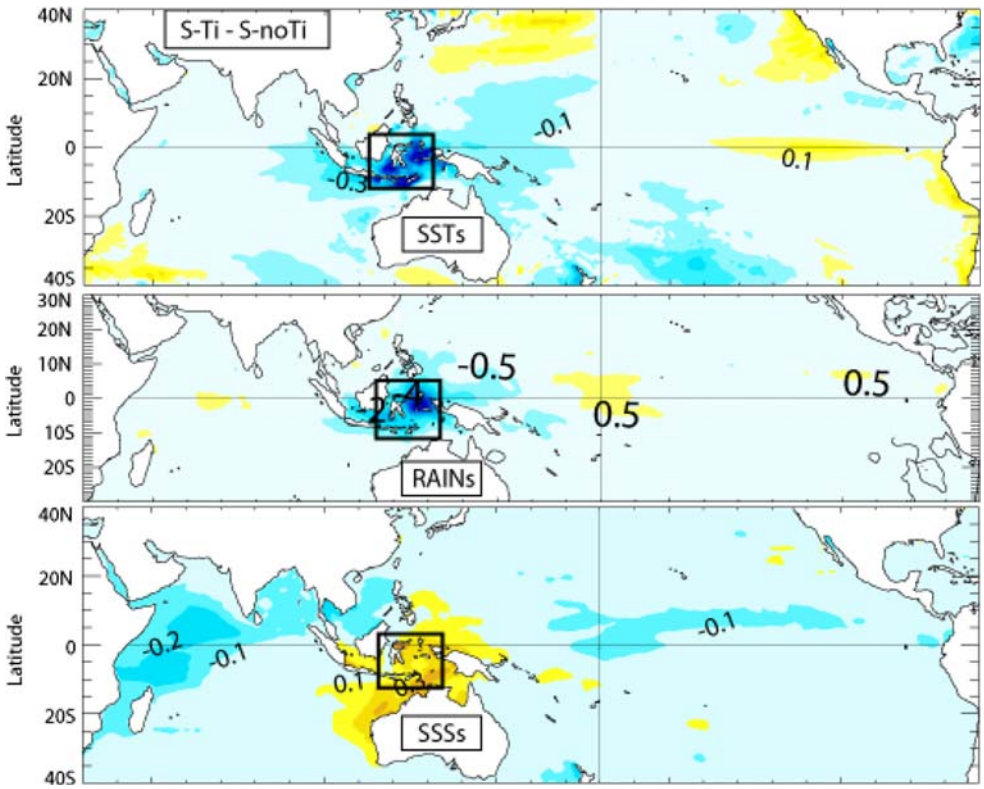

Fig. 9 SST *top*, rain *middle*, SSS *bottom* anomalies between S-Ti and S-noTi experiments. The *black box* shows the Indonesian domain over which averages are computed in Table 2

(Madec 2008; Madec et al. 1998) for the oceanic dynamical core and LIM2 (Timmermann et al. 2005) for sea–ice model. We use the configuration known as "ORCA05" which is a tri-polar global grid with a resolution of 0.5°/ 0.5°cos (latitude). Vertical resolution and mixing are similar to OPA8.2. The atmospheric component is ECHAM5.2 (Roeckner et al. 2003, 2004) with a T106 horizontal resolution and 31 hybrid sigma-pressure levels. A mass flux scheme (Tiedtke 1989) is applied for cumulus convection with modifications for penetrative convection according to Nordeng 1994. The coupling information, without flux correction, is exchanged every two hours by means of the OASIS 3 coupler (Valcke 2006). This higher resolution coupled SINTEX model has been run for 50 years only, due to computational expense.

The surface response to tidal mixing in the SINTEX model is comparable in structure and amplitude to the one found in HadOPA (Fig. 9; Table 2). Locally, the SST and precipitations display the same response in amplitude (−0.5°C, −1.5 mm/day) in better agreement with observations (Table 3). The wind convergence decreasing and the thermocline flattening are comparable in both models. The main differences concern SSS anomaly amplitude. Indeed the structures are similar in both models but the amplitude both local and remote are smaller for the SINTEX model. This presumably due to the subsurface salinity maximum less intense than for the HadOPA model, which bring less salty water in the surface and a smaller anomaly in the subsurface (not shown).

References

Blanke B, Delecluse P (1993) Variability of the tropical Atlantic Ocean simulated by a general circulation model with two different mixed layer physics. J Phys Oceanogr 23:1363–1388

Chang P, Yamagata T, Schopf P, Behera SK, Carton J, Kessler WS, Meyers G, Qu T, Schott F, Shetye S (2006) Climate fluctuations of tropical coupled systems—the role of Ocean dynamics. J Clim 19(20):5122

Clement AC, Seager R, Murtugudde R (2005) Why are there tropical warm pools? J Clim 18:5294–5311

Cravatte S, Madec G, Izumo T, Menkes C, Bozec A (2007) Progress in the 3-D circulation of the eastern equatorial Pacific in a climate ocean model. Ocean Model 17(1):28–48

Davison AC, Hinkley DV (1997) Bootstrap methods and their application. Cambridge University Press, Cambridge, p 582

Ffield A, Gordon AL (1992) Vertical mixing in the Indonesian Thermocline. J Phys Oceanogr 22(2):184–195. doi: 10.1175/1520-0485

Ffield A, Gordon A (1996) Tidal mixing signatures in the Indonesian seas. J Phys Oceanogr 26:1924–1937

Fieux M, Andrie C, Delecluse P, Ilahude AG, Kartavtseff A, Mantisi F, Molcard R, Swallow JC (1994) Measurement within the Pacific-Indian Ocean throughflow region. Deep-Sea Res I 41:1091–1130

Fischer AS, Terray P, Guikyardi E, Gualdi S, Delecluse P (2005) Two independent Triggers for the Indian Ocean/zonal Mode in a coupled GCM. J Clim 18:3428–3449

Gerkema T, Lam F-PA, Maas LRM (2004) Internal tides in the Bay of Biscay: conversion rates and seasonal effects. Deep Sea Res Part II 51:2995–3008

Gordon AL, McClean J (1999) Thermohaline stratification of the Indonesian Seas, model and observations. J Phys Oceanogr 29:198–216

Gordon AL, Susanto RD (2001) Banda Sea surface layer divergence. Ocean Dyn 52:2–10

Gordon AL, Susanto RD, Ffield AL (1999) Throughflow within Makassar Strait. Geophys Res Lett 26:3325–3328

Gregory D, Rowntree PR (1990) A mass flux convection scheme with representation of cloud ensemble characteristics and stability-dependent closure. Mon Weather Rev 118(7):1483–1506

Gregory D, Kershaw R, Inness PM (1997) Parametrization of momentum transport by convection. II: tests in single column and general circulation models. Q J R Meteor Soc 123:1153–1183

Gualdi S, Guilyardi E, Navarra A, Masina S, Delecluse P (2003) The interannual variability in the Tropical Indian Ocean as simulated by a CGCM. Clim Dyn 20:567–582

Hautala S, Reid JL, Bray NA (1996) The distribution and mixing of Pacific water masses in the Indonesian Seas. J Geophys Res 101(C5):12375–12390

Hautala SL, Sprintall J, Potemra JT, Chong JC, Pandoe W, Bray N, Ilahude AG (2001) Velocity structure and transport of the Indonesian Throughflow in the major straits restricting flow into the Indian Ocean. J Geophys Res 106(C9):19527–19546

Hirst AC, Godfrey JS (1993) The role of the Indonesian Throughflow in a global ocean GCM. J Phys Oceanogr 23:1057–1086

Jochum M, Potemra J (2008) Sensitivity of tropical rainfall to Banda Sea diffusivity in the community climate system model. J Clim 21:6445–6454

Kamenkovich VM, Burnett WH, Gordon AI, Mellor GL (2003) The Pacific/Indian Ocean pressure difference and its influence on the Indonesian Seas circulation: Part II—the study with specified sea-surface heights. J Mar Res 61(5):613–634

Koch-Larrouy, Madec G, Bouruet-Aubertot P, Gerkema T, Bessières L, Molcard R (2007) On the transformation of Pacific Water into Indonesian Throughflow water by internal tidal mixing. Geophys Res Lett 34:L04604. doi:10.1029/2006GL028405

Koch-Larrouy A, Madec G, Iudicone D, Molcard R, Atmadipoera A (2008a) Quantification of the mixing process in the transformation of water masses in the Indonesian Seas. Ocean Dyn (submitted)

Koch-Larrouy A, Madec G, Blanke B, Molcard R (2008b) Quantification of the water paths and exchanges in the Indonesian archipelago. Ocean Dyn (submitted)

Lau N-C, Nath MJ (2004) Coupled GCM simulation of atmosphere–ocean variability associated with zonally asymmetric SST changes in the tropical Indian Ocean. J Clim 17:245–265

Lengaigne M, Madec G, Menkes C, Alory G (2003) Impact of isopycnal mixing on the tropical ocean circulation. J Geophys Res 108(C11):3345. doi:10.1029/2002JC001704

Lengaigne M, Guilyardi E, Boulanger JP, Menkes C, Delecluse P, Inness P, Cole J, Slingo J (2004) Triggering of El Niño by westerly wind events in a coupled general circulation model. Clim Dyn 23:601–620. doi:10.1007/s00382-004-0457-2

Lengaigne M, Boulanger JP, Menkes C, Spencer H (2006) Influence of the seasonal cycle on the termination of El Niño events in a coupled general circulation model. J Clim 19:1850–1868. doi:10.1175/JCLI3706.1

Li T, Wang B, Chang CP, Zhang Y (2003) A theory for the Indian Ocean dipole-zonal mode. J Atmos Sci 60:2119–2135

Lin JL (2007) The Double-ITCZ problem in IPCC AR4 coupled GCMs: Ocean–atmosphere feedback analysis. J Clim 20:4497–4525

Luo J-J, Masson S, Behera S, Delecluse P, Gualdi S, Navarra A, Yamagata T (2003) South Pacific origin of the decadal ENSO-like variationas simulated by a coupled GCM. Geophys Res Lett 30(24):2250. doi:10.1029/2003GL018649

Luo J-J, Masson S, Behera S, Yamagata T (2007) Experimental forecasts of Indian Ocean Dipole using a coupled OAGCM. J Clim 20(10):2178–2190

Lyard F et al (2002) Energy budget of the tidal hydrodynamic model fes99. In: C. Le Provosts' talk: "Ocean tides after a decade of high precision satellite altimetry", SWT Jason 1, Arles, 2003

Madec G (2008) "NEMO reference manual, ocean dynamics component: NEMO-OPA. Preliminary version". Note du Pole de modélisation, Institut Pierre-Simon Laplace (IPSL), France, No 27 ISSN No 1288-1619

Madec G, Delecluse P, Imbard M, Lévy C (1998) OPA 8.1 Ocean general circulation model reference manual. Note du Pole de modélisation, Institut Pierre-Simon Laplace (IPSL), France, No 11, 91 pp

Meng X, Wu D, Hu R, Lan J (2004) The interdecadal variation of Indonesian Throughflow and its mechanism. Chin Sci Bull 2004 49(19):2058–2067

Meyers G, Bailey RJ, Worby AP (1995) Geostrophic transport of Indonesian throughflow. Deep-Sea Res Part I 42:1163–1174

Molcard RM, Fieux M, Syamsudin F (2001) The throughflow within Ombai Strait. Deep-Sea Res I 48:1237–1253

Murray SP, Arief D (1988) Throughflow into the Indian Ocean through the Lombok Strait, January 1985–January 1986. Nature 333:444–447

Murtugudde R, Busalacchi AJ, Beauchamp J (1998) Seasonal-to-interannual effects of the Indonesian throughflow on the tropical Indo-Pacific Basin. J Geophys Res 103(21):425–441

Murtugudde R, McCreary J, Busalacchi AJ (2000) Oceanic processes associated with anomalous events in the Indian Ocean with relevance to 1997–98. J Geophys Res 105:3295–3306

Neale R, Slingo J (2003) The maritime continent and its role in the global climate: AGCM study. J Clim 16:834–848

Nordeng TE (1994) Extended versions of the convective parameterization scheme at ECMWF and their impact on the mean and transient activity of the model in the tropics, Tech. Memo. 206. Eur. Cent. for Medium-Range Weather Forecasts, Reading, UK

Pope V, Gallani ML, Rowntree PR, Stratton RA (2000) The impact of new physical parameterizations in the Hadley Centre climate model: HadAM3. Clim Dyn 16:123–146

Potemra JT, Schneider N (2005) Influence of low-frequency Indonesian throughflow transport on temperatures in the Indian Ocean in a coupled model. J Clim (submitted)

Potemra JT, Lukas R, Mitchum GT (1997) Large scale estimation of transport from the Pacific to the Indian Ocean. J Geophys Res 102:27795–27812

Robertson R, Ffield A (2005) M2 baroclinic tides in the Indonesian Seas. Oceanogr 18:62–73

Roeckner E, Bäuml G, Bonaventura L, Brokopf R, Esch M, Giorgetta M, Hagemann S, Kirchner I, Kornblueh L, Manzini E, Rhodin A, Schlese U, Schulzweida U, Tompkins A (2003) The atmospheric general circulation model ECHAM 5. PART I: Model description. MPI-Report 349

Roeckner E, Brokopf R, Esch M, Giorgetta M, Hagemann S, Kornblueh L, Manzini E, Schlese U, Schulzweida U (2004) The atmospheric general circulation model ECHAM5 Part II: Sensitivity of simulated climate to horizontal and vertical resolution. Max Planck Institute for Meteorology, Report No. 354

Saji NH, Goswami BN, Vinayachandran PN, Yamagata T (1999) A dipole mode in the tropical Indian Ocean. Nature 401:360–363

Sasaki H, Nonaka M, Masumoto Y, Sasai Y, Uehara H, Sakuma H (2008) An eddy-resolving hindcast simulation of the quasiglobal ocean from 1950 to 2003 on the Earth Simulator. In: Hamilton

K, Ohfuchi W (eds) High resolution numerical modelling of the atmosphere and ocean, chapter 10. Springer, New York, pp 157–185

Schiller A (2004) Effects of explicit tidal forcing in an OGCM on the water-mass structure and circulation in the Indonesian throughflow region. Ocean Model 6(1):31–49

Schiller A, Fiedler R (2007) Explicit tidal forcing in an ocean general circulation model. Geophys Res Lett 34:L03611. doi: 10.1029/2006GL028363

Schiller A, Godfrey JS, McIntosh PC, Meyers G, Wijffels SE (1998) Seasonal near-surface dynamics and thermodynamics of the Indian Ocean and Indonesian Throughflow in a global ocean circulation model. J Phys Oceanogr 28:2288–2312

Schneider N (1998) The Indonesian Throughflow and the global climate system. J Clim 11:676–689

Song Q, Gordon AL (2004) Significance of the vertical profile of the Indonesian Throughflow transport to the Indian Ocean. Geophys Res Lett 31:L16307. doi:10.1029/2004GL020360

Song Q, Vecchi GA, Rosati AJ (2007) The role of the Indonesian Throughflow in the Indo-Pacific climate variability in the GFDL coupled climate model. J Clim 20(11):2434

Spencer H, Slingo JM (2003) The simulation of peak and delayed ENSO teleconnections. J Clim 16(11):1757–1774

Sprintall J, Wijffels S, Molcard R, Jaya I (2008) Transport variability in the exit passages of the Indonesian Throughflow. J Geophys Res (submitted)

St. Laurent LC, Simmons HL, Jayne SR (2002) Estimates of tidally driven enhanced mixing in the Deep Ocean. Geophys Res Lett 29:101029

Susanto RD, Gordon AL (2005) Velocity and transport of the Makassar Strait Throughflow. J Geophys Res 110, Jan C01005. doi:10.1029/2004JC002425

Terray P, Chauvin F, Douville H (2007) Impact of southeast Indian Ocean sea surface temperature anomalies on monsoon-ENSO-dipole variability in a coupled ocean/atmosphere model. Clim Dyn 28(6):553

Tiedtke M (1989) A comprehensive mass flux scheme for cumulus parameterization in large-scale models. Mon Weather Rev 117:1779–1800

Timmermann R, Goosse H, Madec G, Fichefet T, Ethe C, Duliere V (2005) On the representation of high latitude processes in the ORCA-LIM global coupled sea–ice–ocean model. Ocean Modell 8(2005):175–201

Valcke S (2006) OASIS3 user guide (prism_2-5). PRISM support initiative report No 3, 64 pp

Valcke S, Terray L, Piacentini A (2000) Oasis 2.4, Ocean atmosphere sea ice soil: user's guide. Technical report TR/CMGC/00/10, CERFACS, Toulouse, France

Vialard J, Menkes C, Boulanger J-P, Delecluse P, Guilyardi E, McPhadenet MJ, Madec G (2001) Oceanic mechanisms driving the SST during the 1997–1998 El Niño. J Phys Oceanogr 31:1649–1675

Wajsowicz RC, Schneider EK (2001) The Indonesian throughflow's effect on global climate determined from the COLA coupled climate system. J Clim 14:3029–3042

Wang B (1995) Interdecadal changes in El Nino onset in the last four decades. J Clim 8:267–285

Webster PJ, Moore AM, Loschnigg JP, Leben RR (1999) Coupled ocean–atmosphere dynamics in the Indian Ocean during 1997–98. Nature 401:356–360